Enhanced high temperature thermoelectric properties of Bi-doped *c*-axis oriented $Ca_3Co_4O_9$ thin films by pulsed laser deposition

T. Sun,[1] H. H. Hng,[1] Q. Y. Yan,[1] and J. Ma[1,2,a)]
[1]*School of Materials Science and Engineering, Nanyang Technological University, Singapore 639798*
[2]*Temasek Laboratories, Nanyang Technological University, Singapore 637553*

(Received 11 August 2010; accepted 5 September 2010; published online 21 October 2010)

$Ca_{3-x}Bi_xCo_4O_9$ (x=0–0.4) thin films were deposited on single-crystal sapphire (0001) substrates by pulsed laser deposition. Structural characterizations indicated that these thin films exhibited perfect *c*-axis orientation and were well crystallized. Surface chemical states analysis confirmed Bi-substitution for Ca in the thin films with $x<0.4$. For the thin film with x=0.4, excessive Bi were found isolated within the film. Due to their perfect orientation, in-plane electrical properties of these thin films measured from 300 to 740 K were found to be comparable to those of the single crystals. Furthermore, Bi-substitution was noted for the reduced electrical resistivity and enhanced Seebeck coefficient. The above superior properties resulted in a high power factor of 0.81 mW m^{-1} K^{-2} at 740 K for thin film $Ca_{2.7}Bi_{0.3}Co_4O_9$, which was about 29% improvement as compared to that of pure $Ca_3Co_4O_9$ thin film. The results suggested that Bi-doped $Ca_3Co_4O_9$ thin films could be a promising candidate for thermoelectric applications at elevated temperatures. © *2010 American Institute of Physics*. [doi:10.1063/1.3499324]

I. INTRODUCTION

Thermoelectric (TE) energy conversion is noted to be one of the promising technologies for energy recovery and power generation. It offers a direct way to reclaim the waste heat from systems such as automobiles, which is reckoned to be about 70% of the total primary energy. Among the various TE materials, misfit layered cobalt oxides are considered to be one of the most promising candidates to operate in air at high temperatures. This is due to their superior properties, such as low toxicity, thermal stability and high tolerance to oxidation etc.,[1–3] as compared to traditional intermetallic alloys. Among them, $Ca_3Co_4O_9$ is one of the best TE oxides that exhibits a high temperature TE figure of merit, $ZT=S^2T/(\rho\kappa)$, of 0.83 at 1000 K,[4] where S, T, ρ, and κ are the Seebeck coefficient, absolute temperature, electrical resistivity, and thermal conductivity, respectively, and S^2/ρ gives the power factor. The $Ca_3Co_4O_9$ crystal structure is composed of stacks of CdI_2-type CoO_2 layer alternating with rock-salt-type Ca_2CoO_3 layer along the *c*-axis and can be denoted as $[Ca_2CoO_3]^{RS}[CoO_2]_{1.62}$.[2] Many attempts to improve TE efficiency by doping at Ca site have been reported for bulk $Ca_3Co_4O_9$.[5–9] Particularly, it has been shown that Bi-substitution is effective to increase the Seebeck coefficient while maintaining the electrical resistivity of the system.[7–9]

It is noted that for many advanced applications, large size single crystals of $Ca_3Co_4O_9$ are required. However, because of the strong anisotropy in crystal growth and electrical transport, large size single crystals are difficult to fabricate.[4] On the other hand, randomly oriented $Ca_3Co_4O_9$ ceramics show poor TE performance. Thus, many efforts have been made to improve the texture of $Ca_3Co_4O_9$ ceramics by means of hot-forging,[8] spark plasma sintering,[9] and magnetic alignment[10] processes. Recently, epitaxial or *c*-axis oriented $Ca_3Co_4O_9$ thin films have been successfully prepared by radiofrequency sputtering,[11] pulsed laser deposition (PLD),[12,13] and topotactic ion-exchange method.[14] Due to the perfect crystal orientation, thin film in-plane TE properties were found to be better than the textured bulk ceramics and comparable to the single crystals. The thin film approach can also be applied to TE devices for localized cooling.[15] Furthermore, thin film configuration facilitates further improvement of the TE performance by reducing the thermal conductivity via the lattice mismatches and/or scattering effects in the film, and at the same time, enhances the thermopower through structures such as superlattices or quantum wells.[16] However, thus far, only pure $Ca_3Co_4O_9$ thin films were fabricated and studied. In this work, we report for the first time a study on the effects of Bi-doping in high quality *c*-axis oriented $Ca_3Co_4O_9$ thin films. High temperature electrical properties, which are essential but seldom reported for $Ca_3Co_4O_9$ thin films, will also be investigated. The property improvement by heavy doping into the highly-orientated thin films will open up tremendous opportunities for future TE applications.

II. EXPERIMENTAL SECTION

$Ca_{3-x}Bi_xCo_4O_9$ (x=0, 0.1, 0.2, 0.3, and 0.4, named as CCO, Bi01, Bi02, Bi03, and Bi04 respectively) thin films with *c*-axis orientation were prepared on (0001) sapphire (*c*-plane) single crystal substrates by PLD method. The thin film growth was carried out at substrate temperature of 700 °C in 20 Pa (150 mTorr) oxygen pressure by using a KrF excimer laser (Lambda Physik Compex, $\lambda=248$ nm) with a laser energy density of ~1.2 J/cm^2/pulse and the deposition rate was about ~2 nm/min. The ceramic $Ca_{3-x}Bi_xCo_4O_9$ targets were synthesized as follows: oxides powders with nominal cation ratios (Table I) were first obtained by sol-gel method[9] and then calcined at 700 °C. Due

a)Electronic mail: asjma@ntu.edu.sg.

TABLE I. Chemical compositions of the sol-gel solute, PLD targets, and the films measured by ICP and XPS analysis; and the thickness of the thin films.

Sample name	Nominal composition	Sol-gel solute Ca:Bi:Co	Target Ca:Bi:Co	Film Ca:Bi:Co	Film thickness (nm)
CCO	$Ca_3Co_4O_9$	3:0:4	3.04:0.00:4	3.02:0.00:4	99.8
Bi01	$Ca_{2.9}Bi_{0.1}Co_4O_9$	2.9:0.11:4	2.92:0.12:4	2.87:0.10:4	87.6
Bi02	$Ca_{2.8}Bi_{0.2}Co_4O_9$	2.8:0.22:4	2.84:0.25:4	2.75:0.21:4	97.4
Bi03	$Ca_{2.7}Bi_{0.3}Co_4O_9$	2.7:0.33:4	2.74:0.36:4	2.65:0.32:4	88.4
Bi04	$Ca_{2.6}Bi_{0.4}Co_4O_9$	2.6:0.44:4	2.62:0.47:4	2.54:0.42:4	90.3

to its volatility, additional 10% of Bi was added. The resulting powders were pelletized into 1 in. diameter disks followed by sintering at 880 °C for 20 h. The chemical compositions of the final targets were confirmed by inductively coupled plasma (ICP) analysis using a Dual-view Optima 5300 DV ICP-optical emission spectrometry (OES) system (Perkin Elmer), and the results are shown in Table I. Table I also summarizes the thicknesses of the thin films, which were measured using an Alpha-Step IQ surface profiler. High resolution x-ray diffraction (HRXRD) data were collected using X'Pert MRD (PANalytical) with monochromatic Cu $K\alpha$ radiation ($\lambda = 1.5406$ Å) over 5°–55° range. Surface characterization was performed by an x-ray photoelectron spectroscopy (XPS) using Theta Probe XPS (Thermo Fisher Scientific) equipped with an aluminum anode (15 kV, 100 W, $hv = 1,486.6$ eV) and a quartz monochromator. The C 1*s* peak located at 284.5 eV was assigned to carbon from adventitious contaminations, and was used as the criterion to rectify binding energies of XPS spectra. Transmission electron microscopy (TEM) images and selected-area election diffraction (SAED) patterns were taken using a JEM-2100F (JEOL) at 200 kV. The in-plane electrical resistivity (ρ_{ab}) and Seebeck coefficient (S) of the thin films were measured from room temperature to ~740 K by the standard four-probe method and the conventional steady state method, respectively. Room temperature carrier concentrations (n) of the thin films were determined by the Hall measurement (Bio Rad HL5500) with four-point-probe technique using van der Pauw geometry.

III. RESULTS AND DISCUSSION

Figure 1(a) shows the HRXRD 2θ-ω scans of pure and Bi-doped $Ca_3Co_4O_9$ thin films on (0001) sapphire substrate. Diffraction peaks of $Ca_3Co_4O_9$ are indexed using four integers, h, k, l, and m, with the reciprocal-lattice vectors $\boldsymbol{q}$, from the formula, $\boldsymbol{q} = h\boldsymbol{a}^* + k\boldsymbol{b}_1^* + l\boldsymbol{c}^* + m\boldsymbol{b}_2^*$ according to the reported misfit structure of $Ca_3Co_4O_9$ with $Cm(0\ 1-p\ 0)$ superspace group.[17] Besides the peak from sapphire (0006) substrate, only peaks from diffractions of (00l0) $Ca_3Co_4O_9$ planes are observed, indicating that the film is c-axis oriented. No extra peaks corresponding to any possible secondary phases, such as $Bi_2Ca_2Co_2O_x$,[7] were observed for the Bi-doped $Ca_3Co_4O_9$ thin films. The result reveals that the Bi large ions can be doped into the lattice of $Ca_3Co_4O_9$ within the range $x \leq 0.4$ without any detectable change in the crystal structure. It can be seen that diffraction peaks for the Bi-substituted samples tend to shift toward the lower 2θ angle as compared to that of pure CCO thin film, as shown in the fine scan of the (0040) peaks in Fig. 1(b). Based on the positions of the (00l0) diffraction peaks, the c-axis lattice constants for each sample were calculated. Figure 1(c) shows that the c-axis lattice constants increase gradually with the amount of Bi composition (determined by XPS). This observation is consistent with the reported work on Bi-substituted $Ca_3Co_4O_9$ bulk materials,[7,8] indicating the enlargement of the crystallographic structure due to the larger Bi^{3+} (1.03 Å) substitution for Ca^{2+} (1.00 Å). Figure 2(a) shows the cross-sectional TEM image of the Bi03 thin film, where the atomic misfit layered structure on the sapphire substrate can be seen. Stacking faults and defects observed in the film layer are consistent with that reported for $Ca_3Co_4O_9$ thin films fabricated by PLD.[12,13] The SAED patterns of the film [Fig. 2(b)] and substrate [Fig. 2(c)], taken with the incident electron beam along the same direction, further confirmed the structure and the c-axis growth direction of the $Ca_3Co_4O_9$ thin film. Both TEM image and SAED observation were found to be consistent with the well crystallized $Ca_3Co_4O_9$ thin film with perfect c-axis orientation.

The cation composition in the pure and Bi-doped

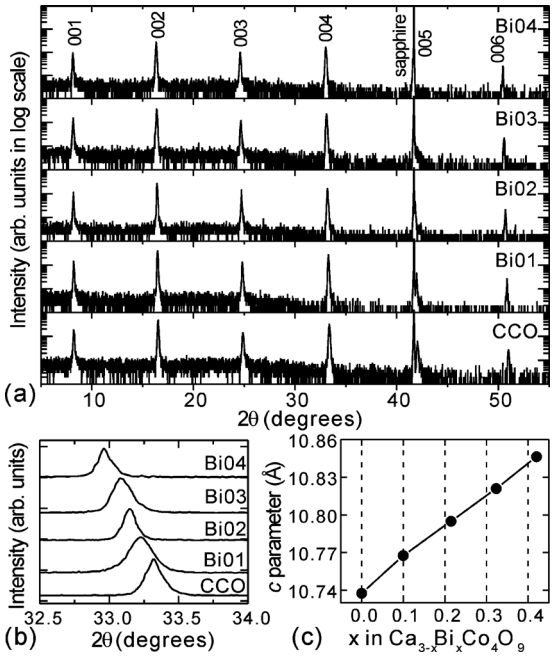

FIG. 1. (a) HRXRD long scan of $Ca_{3-x}Bi_xCo_4O_9$ (x=0, 0.1, 0.2, 0.3, and 0.4) thin films, (b) fine scan of (0040) peaks, and (c) relationship between Bi content determined by XPS and c cell parameter calculated from the 2θ angle of (00l0) peaks.

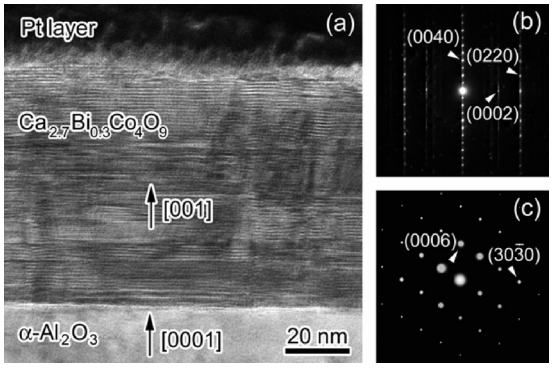

FIG. 2. (a) Cross-sectional TEM image of the Bi03 thin film and the SAED patterns of (b) the Bi03 film and (c) the sapphire substrate.

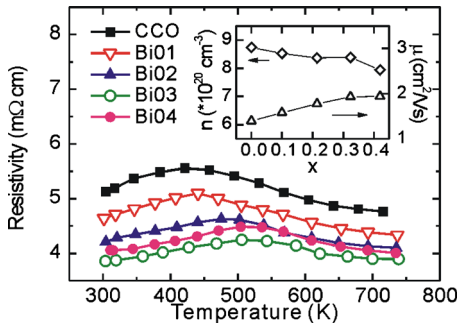

FIG. 4. (Color online) Temperature dependence of in-plane electrical resistivity ρ for $Ca_{3-x}Bi_xCo_4O_9$ (x=0, 0.1, 0.2, 0.3, and 0.4) thin films on sapphire (0001). The inset shows the variations in the carrier concentrations n and the carrier mobility μ with the Bi content.

$Ca_3Co_4O_9$ thin films were investigated by XPS quantitative analysis using the area ratios of Ca $2p_{3/2}$, Co $2p_{3/2}$, and Bi $4f_{7/2}$ peaks and Tougaard-type background after calibration with their sensitivity factors. The calculated thin film compositions (by assigning Co=4.0) are listed in Table I. Due to the volatile nature of Bi, Bi compositions of the thin films were found to be slightly less than their respective targets. However, the resulting amount of Bi in the thin films was still higher than the nominal composition due to the excess Bi initially used to fabricate the targets. In order to determine the Bi chemical states and confirm whether Bi was doped into the $Ca_3Co_4O_9$ structure, XPS fine scans of Bi $4f$ were performed and are shown in Fig. 3. It can be seen that the Bi $4f$ doublets for all the Bi–$Ca_3Co_4O_9$ thin films are located at about 158.3 and 163.6 eV, which are close to the reported Bi^{3+} values.[18] For thin film of Bi04, weak shoulders are observed on the right side of the two peaks at 157.0 and 162.3 eV, which is attributed to isolated Bi. From the XPS result, it is clear that, for thin films with $x<0.4$, most of the Bi atoms are combined with oxygen and have doped into the $Ca_3Co_4O_9$ structure, whereas for the thin film with x=0.4, the Bi content (about 15.2% at Ca site) has gone beyond the doping limit in the $Ca_3Co_4O_9$ structure. Combined with the XRD results, the limit of the Bi-substitution appears to be

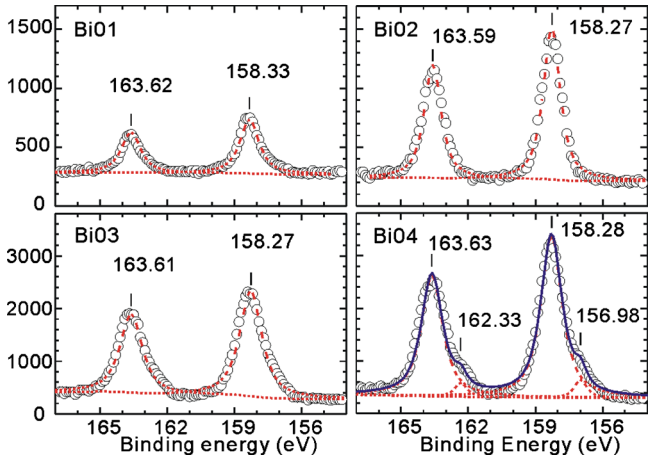

FIG. 3. (Color online) XPS fine scan of Bi $4f$ of Bi-doped $Ca_3Co_4O_9$ thin films. The open circle symbols represent the experimental result while the dashed peaks (with red color online) are fitted peaks. The solid line (with blue color online) is the sum of the fitted peaks for Bi04.

x=0.3 for our PLD fabricated $Ca_3Co_4O_9$ thin films, which is consistent with the limitation of reported Bi-doped $Ca_3Co_4O_9$ single crystals.[7]

Figure 4 shows the in-plane (ab-plane) electrical resistivity (ρ_{ab}) versus temperature (T) for the as-prepared thin films on sapphire (0001). All samples show similar transport behavior with a gradually metal–insulator (MI) transition around 400–550 K. Upon further increase in the temperatures, $\rho(T)$ begins to exhibit semiconductorlike transport behavior. Such MI transition has been observed in many previous reports[3] and is associated with a spin-state transition of Co ions[19] and/or a first-order phase transition of $Ca_3Co_4O_9$ system.[20] The electrical resistivity of the thin film is noted to be about 4–5.5 mΩ cm over the temperature range measured. These ρ values of the thin films are lower than that of most reported $Ca_3Co_4O_9$ ceramics (6–12 mΩ cm),[8–10] and are comparable to those reported for single crystals,[4,7] which confirm the enhancement on electrical transport properties by the highly oriented structure and good quality of the thin films using PLD method. Compared with the pure CCO film, a remarkable reduction in ρ was observed for the Bi-doped films. Similar observation has also been reported for Bi-doped $Ca_3Co_4O_9$ bulk ceramics.[7,8] The electrical resistivity can be expressed as $\rho=1/\sigma=1/(\mu ne)$, where σ, n, and μ are the electrical conductivity, carrier concentration, and carrier mobility, respectively. From Hall effect, R_H, measurements, in-plane n $(=1/eR_H)$, and μ $(=1/\rho ne)$ of the thin films were calculated, as shown in the inset of Fig. 4. It is found that, n of Bi-doped $Ca_3Co_4O_9$ thin films shows a slight decrease with increasing Bi-doping content. According to the misfit layered structure of $Ca_3Co_4O_9$ system, the edge shared $[CoO_2]$ layers are considered to be responsible for the electrical conduction, whereas the rock-salt-type $[Ca_2CoO_3]$ layers are regarded as a charge reservoir to supply carriers into the CoO_2 layers. Trivalent Bi^{3+} substitution for divalent Ca^{2+} in the $[Ca_2CoO_3]$ layers will inject electrons into the conductive $[CoO_2]$ layer. In the condition of a constant oxygen composition, this results in a decreased n, as the carrier of $Ca_3Co_4O_9$ system is hole. Nevertheless, it has been reported that, Bi-substitution can also effectively reduce the oxygen deficiency in $Ca_3Co_4O_9$ phase.[7] The increase oxygen content can enlarge the number of hole carriers and compensate the decrease amount of n by Bi nonequal-valence substitution

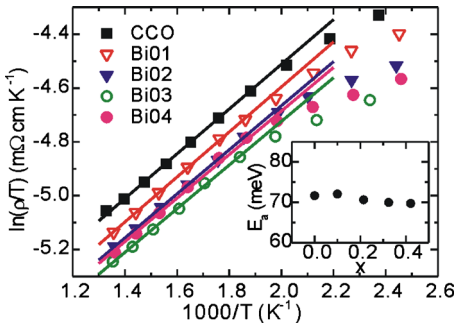

FIG. 5. (Color online) Plot of $\ln(\rho/T)$ vs $1000/T$ for $Ca_{3-x}Bi_xCo_4O_9$ (x=0, 0.1, 0.2, 0.3, and 0.4) thin films. The lines denote the linear fitting. Inset shows the activation energy E_a obtained from the plots.

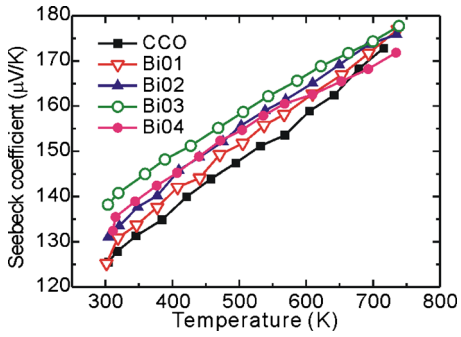

FIG. 6. (Color online) Temperature dependence of in-plane Seebeck coefficient S for $Ca_{3-x}Bi_xCo_4O_9$ (x=0, 0.1, 0.2, 0.3, and 0.4) thin films on sapphire (0001).

for Ca. Therefore, the influence of Bi-substitution on n is reckoned to be not significant, and the reduction in ρ arises from the improvement in μ.

In order to understand the high temperature conduction mechanism, both thermally activated conduction model and adiabatic small polaron hopping conduction (SPHC) model were used to examine the data in the high temperature region, where $T>550$ K. The plots of $\ln(\rho/T)$ versus $1000/T$ for all the samples lie on straight lines above 550 K, as shown in Fig. 5, indicating the SPHC behavior of these thin films. According to the SPHC mechanism[9] of $Ca_3Co_4O_9$, the temperature dependence of electrical resistivity can be generally expressed as

$$\frac{1}{\rho}=\sigma=nea^2\left(\frac{A}{T}\right)\exp\left(\frac{-E_a}{k_BT}\right), \tag{1}$$

where a is the intersite distance of hopping, E_a is the activation energy, k_B is the Boltzmann constant, and A is the pre-exponential terms related to the scattering mechanism. Apart from n, only a and E_a could be influenced by ion substitution. From the slopes of the plots in Fig. 5, E_a is found in the range of 68–72 meV, which is slightly lower than the reported values (77–85 meV) for $Ca_3Co_4O_9$ ceramics.[21] It is reported that grain boundaries and interfaces can act as an energy filter and eliminate the lower energy carriers.[22] As a result, random orientation, small crystal size and/or more structural defects will result in larger activation energy. As confirmed in the earlier analysis, our pure and Bi-doped $Ca_3Co_4O_9$ thin films show good crystallization and perfect c-axis orientation. Hence, smaller amount of grain boundaries and interfaces can be expected. This, in turn, will contribute to the reduction in E_a. PLD method has thus shown its advantage to facilitate the forming of $Ca_3Co_4O_9$ thin films with lower electrical resistivity than ceramics obtained by conventional solid state processing method. Furthermore, it is found that, for all the thin film samples, E_a is almost independent of the Bi-substitution. This is consistent with the above mentioned mechanism that, Bi-substitution at the $[Ca_2CoO_3]$ layers does not change the hopping process, which happened at the $[CoO_2]$ layers. Therefore, the reduction in ρ in Bi-substituted $Ca_3Co_4O_9$ thin films should be attributed to the change in a. As shown in the earlier XRD result, Bi-substitution with larger ion diameter enlarges the lattice constant of $Ca_3Co_4O_9$. This provides a direct influence on the intersite distance of hopping.[9] Moreover, Bi-substitution is helpful to moderate the misfit relation of the $[Ca_2CoO_3]$ and the $[CoO_2]$ subsystems and eliminate structural defects and stacking faults, thereby reduces the scattering of hole carriers and increases a.[8] In conclusion, although Bi^{3+} substitution for Ca^{2+} is noted to decrease the p-type carrier concentration, the electrical resistivity of the thin films can still be reduced by the increase in carrier mobility from the increased intersite distance of hopping.

The temperature dependences of Seebeck coefficient (S) for the pure and Bi-doped $Ca_3Co_4O_9$ thin films are presented in Fig. 6. All the samples show a positive S over the entire temperature range (300–740 K) indicating that major carriers in these thin film samples are holes, which is in agreement with the Hall effect measurements. Compared with pure CCO thin film, S of the $Ca_{3-x}Bi_xCo_4O_9$ ($x<0.4$) thin films increases with Bi content and shows a similar temperature dependence. For the Bi03 thin film, S reaches ~177 μV/K at ~740 K, which is similar to that of the Bi-doped $Ca_3Co_4O_9$ single crystals.[7] In the $Ca_3Co_4O_9$ system, S can be expressed by the Mott formula,[21,23]

$$S(T)=\frac{1}{eT}\frac{\int_{-\infty}^{\infty}\sigma(\varepsilon)(\varepsilon-\mu)\frac{\partial f(\varepsilon)}{\partial\varepsilon}d\varepsilon}{\int_{-\infty}^{\infty}\sigma(\varepsilon)\frac{\partial f(\varepsilon)}{\partial\varepsilon}d\varepsilon}, \tag{2}$$

where $\sigma(\varepsilon)$ and $f(\varepsilon)$ represent electrical conductivity and Fermi–Dirac distribution function at energy ε. The product of the TE coefficient and temperature can be, therefore, understood as a mean energy flow carried by a conduction electron. By using the condition of $\partial f(\varepsilon)/\partial\varepsilon=\delta(\varepsilon=E_F)$, and $\sigma=en\mu(\varepsilon)$,[21,23] Eq. (2) can be written as:

$$S(T)=\frac{c_e}{n}+\frac{\pi^2k_B^2T}{3e}\left[\frac{\partial\ln\mu(\varepsilon)}{\partial\varepsilon}\right]_{\varepsilon=E_F}, \tag{3}$$

where $\mu(\varepsilon)$, c_e, and k_B are energy correlated carrier mobility, electronic specific heat, and Boltzmann constant, respectively. In the $Ca_3Co_4O_9$ system, the first term of Eq. (3) is considered to be dominant, similar with the Drude picture $S\sim c_e/n$. As discussed above, the carrier concentration n decreases with the increase in Bi-doping content. So the change in S can generally be explained by the variation in n. For the Bi04 thin film, S is lower than that of Bi03 sample, and

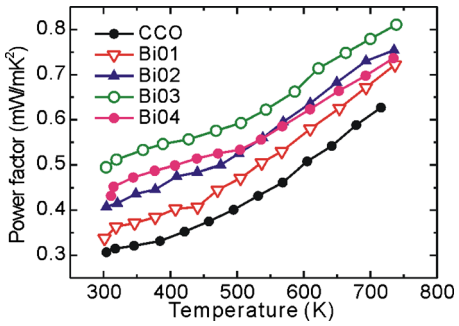

FIG. 7. (Color online) Temperature dependence of power factor P for $Ca_{3-x}Bi_xCo_4O_9$ (x=0, 0.1, 0.2, 0.3, and 0.4) thin films on sapphire (0001).

shows even lower S than pure CCO thin film at high temperature above 700 K. This may be due to the excessive Bi isolated in the thin film, which are contributing as n-type minority carriers. The power factors, P, of the present thin films are calculated from the measured ρ and S, as shown in Fig. 7. The thin film sample of Bi03 is noted to show the highest P value over the temperature range investigated. The thin film power factor has improved by ~29% and reached ~0.81 mW m^{-1} K^{-2} at 740 K compared to pure $Ca_3Co_4O_9$. Moreover, due to their perfect orientation, Bi-doped $Ca_3Co_4O_9$ thin films shows higher power factor than Bi-doped poly crystalline ceramics (~0.5 mW m^{-1} K^{-2}).[8] This huge enhancement on the power factor indicates the great potential of doped $Ca_3Co_4O_9$ materials for TE thin film devices.

IV. CONCLUSION

In summary, Bi-doped $Ca_3Co_4O_9$ thin films were prepared by PLD method using Bi-mixed $Ca_3Co_4O_9$ ceramic targets. The thin films were well crystallized with perfect c-axis orientation. Bi could be successfully doped into the $Ca_3Co_4O_9$ crystal lattice structure for the thin films $Ca_{3-x}Bi_xCo_4O_9$ ($x<0.4$). For the thin film x=0.4, the Bi content was found to exceed the doping limit and resulted in isolated Bi within the film. By using the PLD method, the in-plane electrical properties of the pure and Bi-doped $Ca_3Co_4O_9$ thin films, measured from room temperature to ~740 K, were found to be comparable to that reported for single crystals. Moreover, Bi-substitution at Ca site can effectively increase carrier mobility, hence reduce the electrical resistivity, and Seebeck coefficient of the thin films can be improved simultaneously. As a result, the highest power factor of Bi03 sample reached 0.81 mW m^{-1} K^{-2} at 740 K, suggesting that Bi-doped $Ca_3Co_4O_9$ thin films could be a promising candidate for TE applications at elevated temperatures.

[1] I. Terasaki, Y. Sasago, and K. Uchinokura, Phys. Rev. B **56**, R12685 (1997).
[2] A. C. Masset, C. Michel, A. Maignan, M. Hervieu, O. Toulemonde, F. Studer, B. Raveau, and J. Hejtmanek, Phys. Rev. B **62**, 166 (2000).
[3] R. Funahashi and I. Matsubara, Appl. Phys. Lett. **79**, 362 (2001).
[4] M. Shikano and R. Funahashi, Appl. Phys. Lett. **82**, 1851 (2003).
[5] Y. Wang, Y. Sui, J. G. Cheng, X. J. Wang, and W. H. Su, J. Phys.: Condens. Matter **19**, 356216 (2007).
[6] G. J. Xu, R. Funahashi, M. Shikano, I. Matsubara, and Y. Q. Zhou, Appl. Phys. Lett. **80**, 3760 (2002).
[7] M. Mikami, K. Chong, Y. Miyazaki, T. Kajitani, T. Inoue, S. Sodeoka, and R. Funahashi, Jpn. J. Appl. Phys., Part 1 **45**, 4131 (2006).
[8] M. Mikami, N. Ando, E. Guilmeau, and R. Funahashi, Jpn. J. Appl. Phys., Part 1 **45**, 4152 (2006).
[9] Y. H. Liu, Y. H. Lin, L. Jiang, C. W. Nan, and Z. J. Shen, J. Electroceram. **21**, 748 (2008).
[10] Y. Q. Zhou, I. Matsubara, S. Horii, T. Takeuchi, R. Funahashi, M. Shikano, J. Shimoyama, K. Kishio, W. Shin, N. Izu, and N. Murayama, J. Appl. Phys. **93**, 2653 (2003).
[11] A. Sakai, T. Kanno, S. Yotsuhashi, A. Odagawa, and H. Adachi, Jpn. J. Appl. Phys., Part 2 **44**, L966 (2005).
[12] T. Sun, J. Ma, Q. Y. Yan, Y. Z. Huang, J. L. Wang, and H. H. Hng, J. Cryst. Growth **311**, 4123 (2009).
[13] Y. F. Hu, E. Sutter, W. D. Si, and Q. Li, Appl. Phys. Lett. **87**, 171912 (2005).
[14] K. Sugiura, H. Ohta, K. Nomura, M. Hirano, H. Hosono, and K. Koumoto, Appl. Phys. Lett. **89**, 032111 (2006).
[15] R. Venkatasubramanian, E. Siivola, T. Colpitts, and B. O'Quinn, Nature (London) **413**, 597 (2001).
[16] L. D. Hicks and M. S. Dresselhaus, Phys. Rev. B **47**, 12727 (1993).
[17] Y. Miyazaki, M. Onoda, T. Oku, M. Kikuchi, Y. Ishii, Y. Ono, Y. Morii, and T. Kajitani, J. Phys. Soc. Jpn. **71**, 491 (2002).
[18] W. B. Luo, J. Zhu, Y. R. Li, X. P. Wang, D. Zhao, J. Xiong, and Y. Zhang, Appl. Phys. Lett. **91**, 082501 (2007).
[19] J. Sugiyama, J. H. Brewer, E. J. Ansaldo, H. Itahara, K. Dohmae, Y. Seno, C. Xia, and T. Tani, Phys. Rev. B **68**, 134423 (2003).
[20] J. G. Cheng, Y. Sui, Y. Wang, X. J. Wang, and W. H. Su, Appl. Phys. A: Mater. Sci. Process. **94**, 911 (2009).
[21] Y. Wang, Y. Sui, X. J. Wang, W. H. Su, and X. Y. Liu, J. Appl. Phys. **107**, 033708 (2010).
[22] Y. Q. Zhou, I. Matsubara, W. S. Shin, N. Izu, and N. Murayama, J. Appl. Phys. **95**, 625 (2004).
[23] T. Takeuchi, T. Kondo, T. Takami, H. Takahashi, H. Ikuta, U. Mizutani, K. Soda, R. Funahashi, M. Shikano, M. Mikami, S. Tsuda, T. Yokoya, S. Shin, and T. Muro, Phys. Rev. B **69**, 125410 (2004).